



# Submerged Fatigue Testing of Marine Energy Advanced Materials

## Preprint

Ariel F. Lusty, Paul Murdy, and Julia Gionet-Gonzales

*National Renewable Energy Laboratory*

*Presented at SAMPE 2024  
Long Beach, California  
May 20–23, 2024*

**NREL is a national laboratory of the U.S. Department of Energy  
Office of Energy Efficiency & Renewable Energy  
Operated by the Alliance for Sustainable Energy, LLC**

This report is available at no cost from the National Renewable Energy Laboratory (NREL) at [www.nrel.gov/publications](http://www.nrel.gov/publications).

Contract No. DE-AC36-08GO28308

**Conference Paper**  
NREL/CP-5700-88537  
April 2024



# Submerged Fatigue Testing of Marine Energy Advanced Materials

## Preprint

Ariel F. Lusty, Paul Murdy, and Julia Gionet-Gonzales

*National Renewable Energy Laboratory*

### Suggested Citation

Lusty, Ariel F., Paul Murdy, and Julia Gionet-Gonzales. 2024. *Submerged Fatigue Testing of Marine Energy Advanced Materials: Preprint*. Golden, CO: National Renewable Energy Laboratory. NREL/CP-5700-88537. <https://www.nrel.gov/docs/fy24osti/88537.pdf>.

**NREL is a national laboratory of the U.S. Department of Energy  
Office of Energy Efficiency & Renewable Energy  
Operated by the Alliance for Sustainable Energy, LLC**

This report is available at no cost from the National Renewable Energy Laboratory (NREL) at [www.nrel.gov/publications](http://www.nrel.gov/publications).

Contract No. DE-AC36-08GO28308

**Conference Paper**  
NREL/CP-5700-88537  
April 2024

National Renewable Energy Laboratory  
15013 Denver West Parkway  
Golden, CO 80401  
303-275-3000 • [www.nrel.gov](http://www.nrel.gov)

## NOTICE

This work was authored by the National Renewable Energy Laboratory, operated by Alliance for Sustainable Energy, LLC, for the U.S. Department of Energy (DOE) under Contract No. DE-AC36-08GO28308. Funding provided by U.S. Department of Energy Office of Energy Efficiency and Renewable Energy Water Power Technologies Office. The views expressed herein do not necessarily represent the views of the DOE or the U.S. Government. The U.S. Government retains and the publisher, by accepting the article for publication, acknowledges that the U.S. Government retains a nonexclusive, paid-up, irrevocable, worldwide license to publish or reproduce the published form of this work, or allow others to do so, for U.S. Government purposes.

This report is available at no cost from the National Renewable Energy Laboratory (NREL) at [www.nrel.gov/publications](http://www.nrel.gov/publications).

U.S. Department of Energy (DOE) reports produced after 1991 and a growing number of pre-1991 documents are available free via [www.OSTI.gov](http://www.OSTI.gov).

*Cover Photos by Dennis Schroeder: (clockwise, left to right) NREL 51934, NREL 45897, NREL 42160, NREL 45891, NREL 48097, NREL 46526.*

NREL prints on paper that contains recycled content.

# **SUBMERGED FATIGUE TESTING OF MARINE ENERGY ADVANCED MATERIALS**

Ariel F. Lusty, Paul Murdy, Julia A. Gionet-Gonzales  
National Renewable Energy Laboratory  
Arvada, CO

## **ABSTRACT**

Marine energy structures are typically made of advanced composite materials and are subjected to extreme ocean environments in service. In extreme ocean environments, seawater currents and waves load structures repeatedly, which cause two environmental conditions: water intrusion and mechanical fatigue. In prior research, the two environmental conditions were applied sequentially, where composite specimens were aged and then mechanically tested. To understand the combined effects of dynamic loading and water intrusion on composite materials, the present study involves the static and fatigue four-point bend testing of composite coupons in a water tank. The water tank was designed and built to fit either a 100 kN or a 250 kN load frame. Flexural strength value, cycles to failure, and failure mode results from submerged fatigue testing will be used to inform marine energy structure designs. The coupon-scale test method will be used to scale up to and inform methods for subsequent subcomponent testing and standards development. The benefits of designing marine energy structures to informed standards are decreased lifetime costs and increased reliability and energy production, ultimately leading to a sustainable and low-carbon energy system.

Keywords: composite materials, fatigue testing, marine energy materials  
Corresponding author: Ariel F. Lusty

## **1. INTRODUCTION**

Marine energy devices hold the potential for significant deployment along densely populated coasts [1]. Marine energy includes any kinetic energy inherent to a moving fluid, such as wave or flowing water [2], and marine energy devices are structures that convert this energy into electricity. Marine energy devices have multiple design configurations, including surging flap, floating hull point absorber, axial-flow, and cross-flow turbines. No matter the configuration, marine energy devices must withstand significant periodic loading due to waves, currents, and interactions with the power take-off and control systems. Composite materials are being considered in marine energy device designs for potential strength, weight, and durability benefits [3].

This study involved measuring the combined effects of water intrusion and mechanical fatigue of composite materials. In previous studies such as Meng et al [4], Murdy et al [5], and Jiang et al [6], composites were exposed to moisture and then mechanically fatigue tested. Water ingress had a negative impact on composite fatigue life in each study. Marine energy converters in the field, however, are simultaneously underwater and repeatedly loaded by currents and waves,

which may lead to a further diminishment of composite fatigue life. To simulate the environmental conditions that marine energy converters experience in the field, composites were simultaneously submerged and mechanically fatigue loaded to measure the effects of the two environmental conditions on the fatigue life.

The fatigue life of a specimen consists of three phases. In the first phase, initial fatigue damage produces crack initiation. In the second phase, one or multiple cracks result in the partial separation of a cross section of a specimen. In the third phase, the specimen fractures [7]. A crack will not grow as long as  $G \leq G_c$ , where  $G$  (Equation 1) is the elastic energy release rate and  $G_c$  (Equation 2) is the fracture toughness [8]. The external stress is  $\sigma$ , the failure stress is  $\sigma_c$ , the modulus is  $E$ , and the crack length is  $a$  [7].

$$G = \frac{\pi \sigma^2 a}{E} \quad [1]$$

$$G_c = \frac{\pi \sigma_c^2 a}{E} \quad [2]$$

As a specimen is repeatedly loaded, cracks open and close. In an experimental design where specimens are aged and mechanically loaded sequentially, any water within cracks can be squeezed out into the surroundings. When composites are submerged and cracks open, water enters cracks by capillary motion and is not squeezed out into the surroundings when cracks close [9]. Air is compressible but water is not, so the presence of water within cracks in the specimens leads to increased external stress on the material when cracks close. The increased external stress on cracks leads to increased  $G$  values, which will lead to increased overall crack growth in specimens as  $G$  reaches  $G_c$ . Consequently, increased overall crack growth leads to lower specimen fatigue lives [10].

To measure the effects of water ingress and mechanical fatigue, composite materials were tested in a tank using four-point bend static and fatigue tests. The composites studied were glass fiber reinforced vinyl ester-epoxy and thermoplastic. The tank was designed, constructed, and installed in a 250 kN load frame. In the following sections, flexural strength values, cycles to failure, and failure modes are reported, and results, conclusions, and future work are discussed.

## 2. EXPERIMENTATION

### 2.1 Materials

Two fiberglass [0]<sub>2</sub> composite panels were manufactured using the vacuum assisted resin transfer molding (VARTM) technique at NREL's Composites Manufacturing Education and Technology (CoMET) facility. The panels were manufactured using two layers of Vectorply E-QX 9000 fabric (Figure 1), which was quadriaxial (0, 45, 90, -45) and had a ply thickness of 1.92 mm. Panel dimensions were 34 cm x 90 cm. A different resin system was used for each panel. The resin systems used were Derakane 411C-350 vinyl ester-epoxy and Arkema Elium 188-O, an acrylic-based liquid infusible thermoplastic system. For simplicity, the vinyl ester-epoxy will be termed vinyl ester and the acrylic-based liquid infusible thermoplastic system will be termed thermoplastic. The glass fiber and vinyl ester products were selected to replicate the materials

used in the subcomponent testing for marine energy applications in [5]. The thermoplastic was selected for its recyclability and manufacturability, as demonstrated in [11] and [12], respectively. Vinyl ester is a thermoset polymer. Thermoset polymers are typically densely cross-linked, whereas thermoplastics contain physical cross-links rather than chemical cross-links. A physical cross-link is a non-covalent bond that is stable under one condition but not another [13]. The volume fractions for the vinyl ester and thermoplastic panels were 57% and 58%, respectively. Panels were cut into 15 mm x 175 mm coupons (Figure 2) and visually inspected for manufacturing defects. No defects were observed.

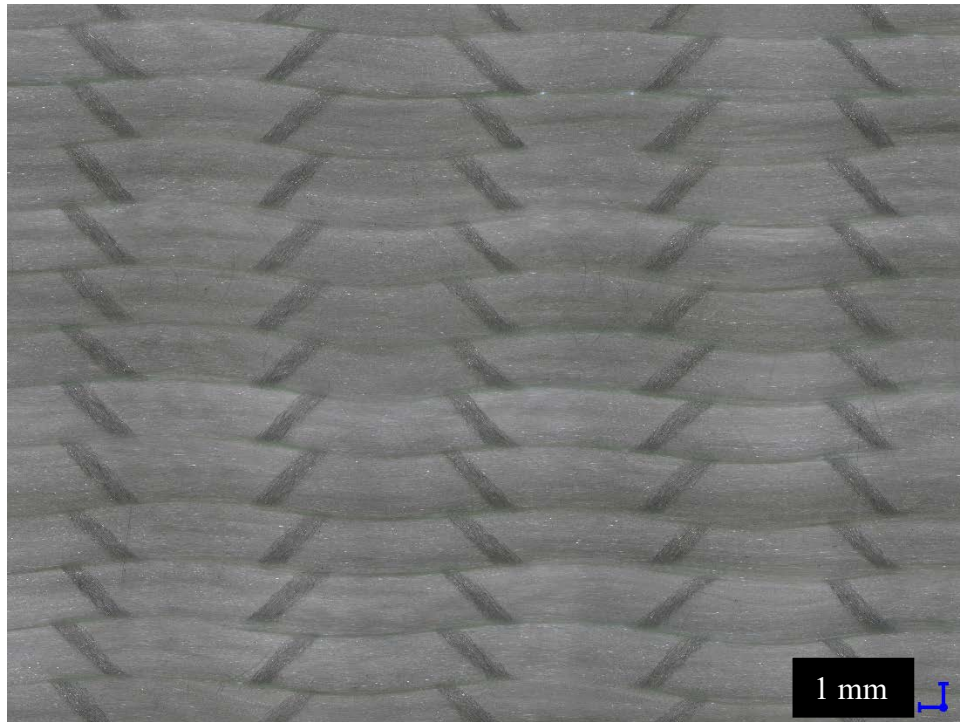


Figure 1. Microscope image of the Vectorply E-QX 9000 fabric.



Figure 2. a) Vinyl ester composite coupon. b) Thermoplastic composite coupon.

The unidirectional tows in the Vectorply E-QX 9000 fabric were wavier than expected. Five fiber waviness angles,  $\theta_w$  (Figure 3), were measured using the image in Figure 1 in Adobe

Photoshop. The average, maximum, and minimum fiber waviness angles were  $7.6^\circ \pm 1.4^\circ$ ,  $8.9^\circ$ , and  $5.2^\circ$ , respectively. The fiber waviness measurement method used in this study was developed based on the method used in Lerman et al [14] to measure the fiber misalignment angle of groups of unidirectional tows. High fiber waviness was observed across multiple rolls of the fabric.

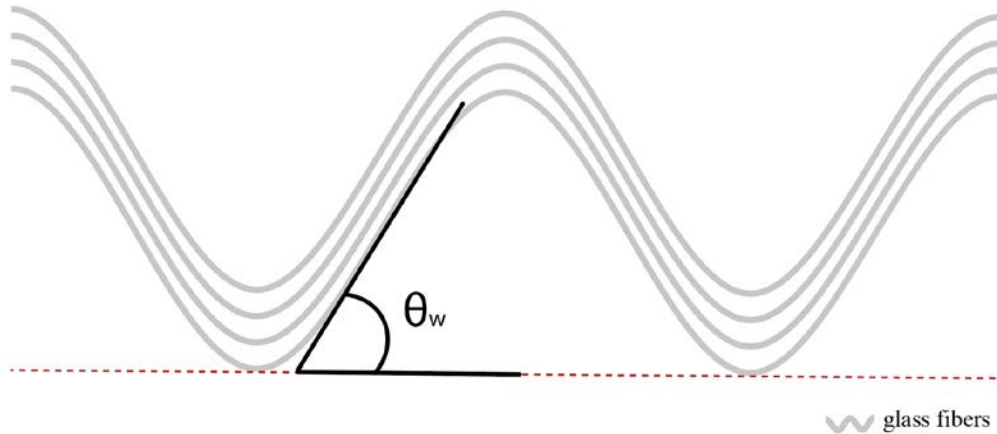


Figure 3. The fiber waviness angle ( $\theta_w$ ) measurement method used for one tow.

As a result of using the VARTM manufacturing technique, the composite panels had smooth and rough sides. The smooth sides are those that were in contact with the glass mold and the rough sides are those that were in contact with the peel ply and vacuum bag. Two  $350\Omega$  strain gauges were adhered to coupons using M-Bond AE-10 epoxy strain gauge adhesive. For the coupons that were fatigue tested underwater, one strain gauge was placed in the center of the rough side and the other was placed in the center of the smooth side (Figure 4). Strain results will not be reported in this publication but will be reported in future work.

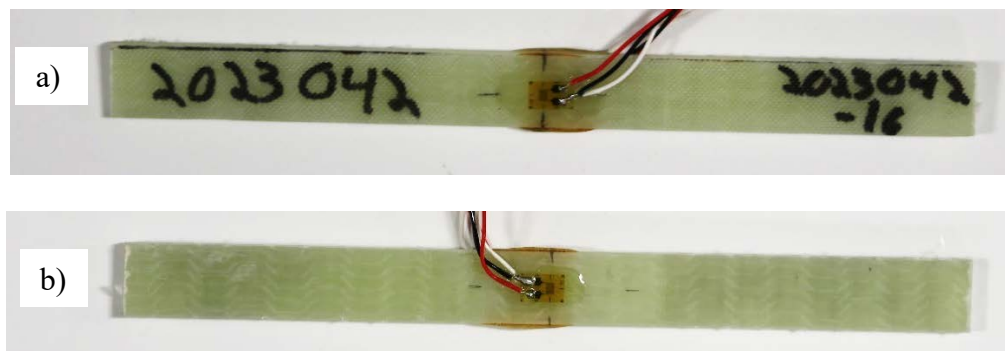


Figure 4. Strain gauge locations on a thermoplastic composite coupon, where a) is the rough side and b) is the smooth side.

## 2.2 Load Frame Setup

Coupons were four-point bend tested in a load frame equipped with a water tank, an anti-rotation kit, and a secondary containment tank. The ASTM D72264 Standard Test Method for Flexural Properties of Polymer Matrix Composite Materials was used as a guide for submerged fatigue four-point bend testing procedure development. The design criteria for the water tank included:

- Usable in both NREL's 100 kN and 250 kN load frames.
- Connected to the actuator along the loading axis.
- Contains a Wyoming Test Fixtures four-point bending fixture.
- Can hold enough water such that test specimens are fully submerged.

The bending fixture had a support span of 140 mm and a load span of 70 mm. The secondary containment tank was designed to protect integrated load frame controls and servo-valves from potential water leaks. The tanks were designed in SolidWorks. The water tank was designed and built with polycarbonate walls and an aluminum base. The base and the walls of the secondary containment tank were designed and built with polycarbonate. The base of the bending fixture was sealed to the base of the water tank with an O-ring and silicone sealant. All corners of the primary and secondary containers were sealed with clear, marine-grade silicone to prevent leaks. The tank was built and installed in a 250 kN load frame (Figure 5).



Figure 5. Photo of the as-built and installed load frame assembly in the 250 kN load frame.



### 2.3 Static Testing Procedure

Five coupons of each resin type were static-tested at 2 mm/min load rate using the load frame setup in Section 2.2. Specimens were placed in the load fixture smooth side-down such that the rough side was in compression and the smooth side was in tension during loading. Specimens were not submerged under water for static testing. MTS TestSuite was used to record load and actuator displacement data. Failure loads were recorded. The maximum flexural stress values were calculated using Equation 3 [15].

$$\sigma = \frac{3PL}{4bh^2} \quad [3]$$

where  $\sigma$  is the maximum flexural stress (MPa),  $P$  is the applied force (N),  $L$  is the support span (mm),  $b$  is coupon width (mm), and  $h$  is the coupon thickness (mm).

### 2.4 Fatigue Testing Procedure

Five coupons of each resin type were fatigue-tested at 75% of the static flexural strength average of the thermoplastic composites, or 497.3 MPa, at 0.65 Hz until failure. A 250kN MTS load frame was used. An R-value of 0.1 was used, where the R-value is the quotient of the applied minimum and maximum stress values.

For submerged tests, food-grade grease was used on the rollers. For dry tests, specimens were not submerged in water, and lithium grease was used on the rollers. For submerged tests, the tank was filled with fresh tap water until the specimen was completely submerged. Like static testing, specimens were placed in the load fixture smooth side-down. Specimens were centered so that the strain gauges were halfway along the load span.

The flexural strength values from static testing were used to compute the applied forces needed for fatigue testing. Equation 4 was subsequently used to compute the setpoints and amplitudes, which were entered into the MTS station manager software. Bespoke, LabVIEW-based data acquisition software was used to record microstrain values, number of cycles, loads, and displacements.

## 3. RESULTS

### 3.1 Static Testing Results

The flexural strength values from static testing are in Table 1.

Table 1. Flexural strength results from static testing.

<b>Material</b>	<b>Flexural Strength (MPa)</b>
<b>Vinyl ester Composite</b>	693.4 ± 21.2
<b>Thermoplastic Composite</b>	663.1 ± 29.0

The flexural strength of the vinyl ester composites was 5% higher than the thermoplastic composites. After failure, both the vinyl ester and the thermoplastic composites had top ply delamination along the gauge section of the compression side (Figure 6).

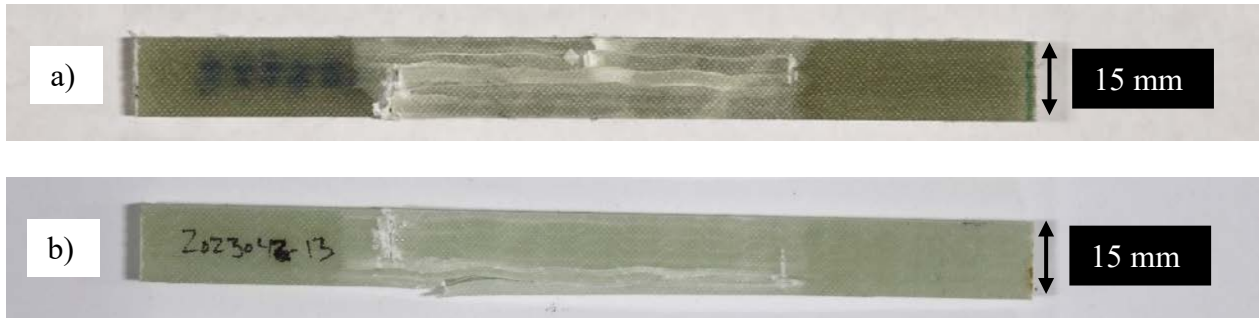


Figure 6. Photos of the compression side top ply delamination after static four-point bend testing for a) vinyl ester and b) thermoplastic coupons.

### 3.2 Fatigue Testing Results

Fatigue testing results are given in Figure 7 and summarized in Table 2.

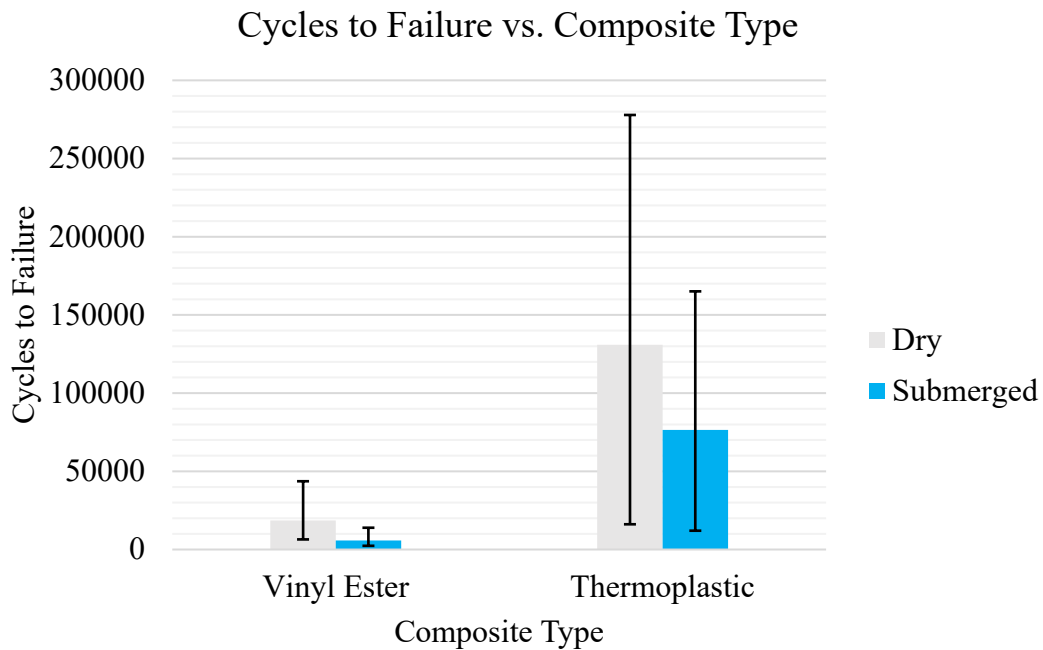


Figure 7. Cycles to failure for vinyl ester and thermoplastic composite dry and fatigue-tested specimens.

Table 2. Fatigue testing results.

Material	Submersion	Cycles to Failure
Vinyl ester composite	Dry	18,593 ± 12,932
	Submerged	5,780 ± 4,745
Thermoplastic composite	Dry	130,863 ± 32,285
	Submerged	76,523 ± 24,065

For dry fatigue tests, the thermoplastic composites had 86% higher cycles to failure than the vinyl ester composites. There were 69% and 42% decreases in cycles to failure from dry to submerged for the vinyl ester and thermoplastic composites, respectively. Both dry vinyl ester and thermoplastic composites had tension-side face sheet delamination (Figures 8 and 9). However, the delamination was more severe in the vinyl ester specimens (Figure 8-b) than the thermoplastic specimens (Figure 9-b).

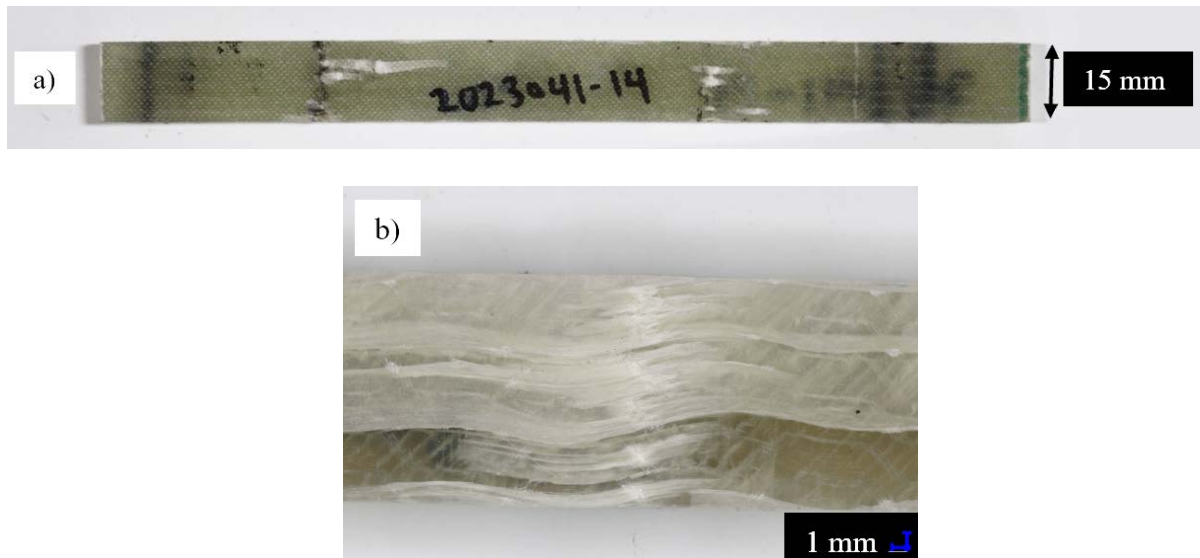


Figure 8. A dry fatigue-tested vinyl ester specimen after failure at 8,901 cycles, where a) is a photo of the compression side and b) is a microscope image at 3.7x magnification of the tension side.

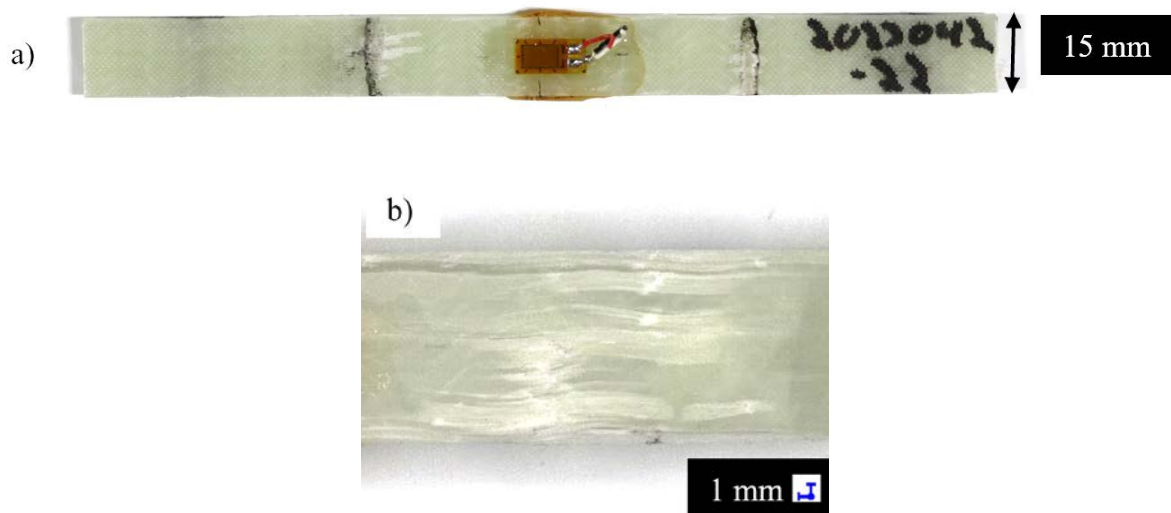


Figure 9. A dry fatigue-tested thermoplastic specimen after failure at 138,435 cycles, where a) is a photo of the compression side and b) is a microscope image at 3.7x magnification of the tension side.

Compared to dry, the submerged vinyl ester specimens had more permanent changes in shape and more fiber breakage on the tension sides (Figure 10). In addition, dry vinyl ester specimens had more delamination near the supports while submerged vinyl ester specimens had more delamination in the gauge section. Both dry and submerged vinyl ester failed specimens had through-thickness delamination. However, the dry vinyl ester specimens had more fiber bridging through the thickness.

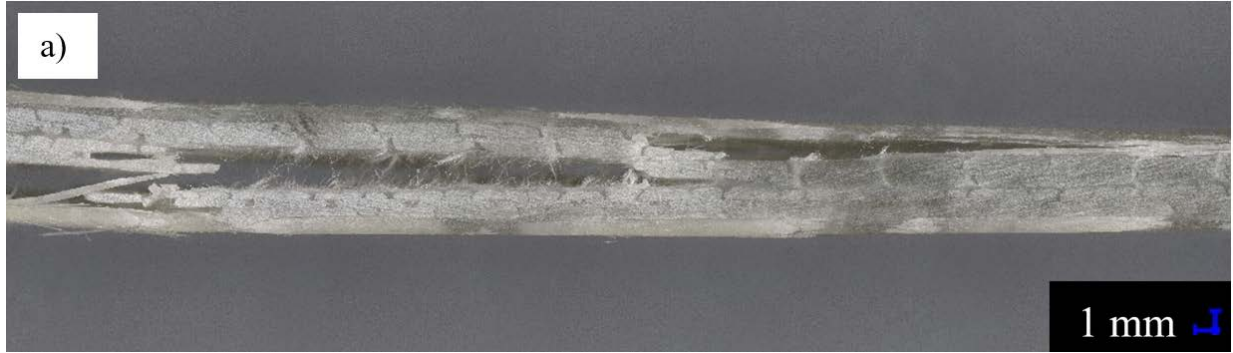


Figure 10. Microscope images at 3.7x magnification of two vinyl ester specimens that were a) dry fatigue-tested and failed at 17,418 cycles and b) fatigue-tested while submerged and failed at 13,125 cycles.

For the thermoplastic specimens, there was more through-thickness delamination failure for dry specimens while there was no through-thickness failure for submerged specimens (Figure 11). Submerged thermoplastic specimens had top-ply delamination failure (Figure 11-b).

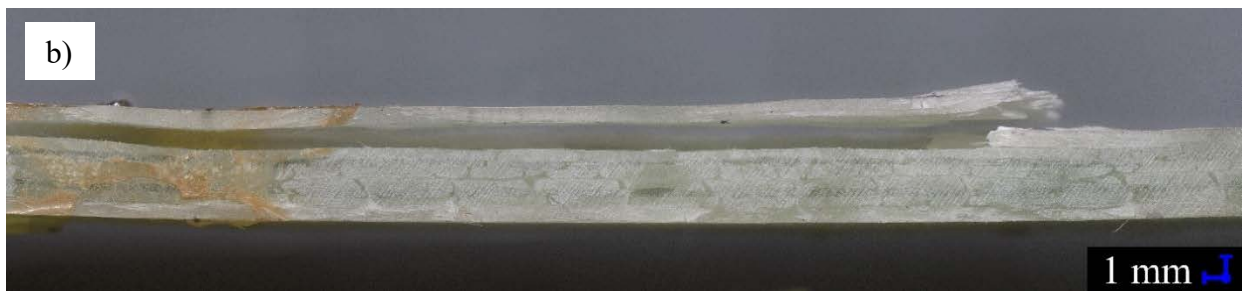
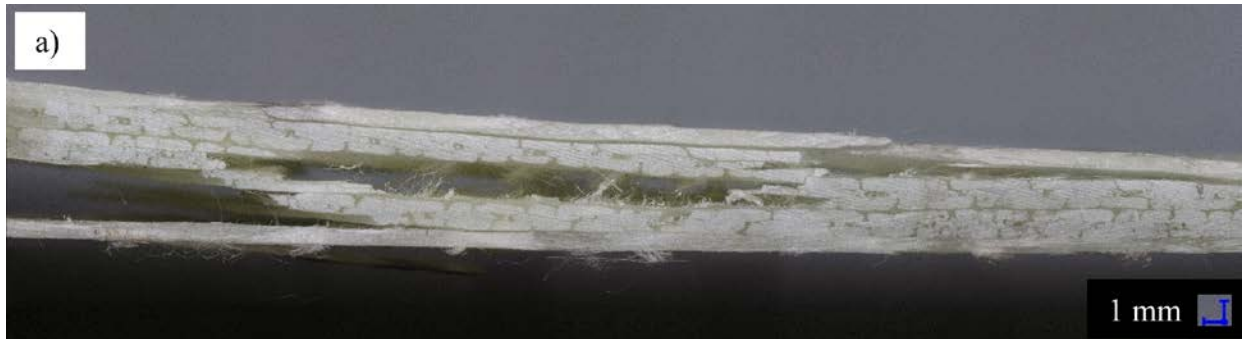


Figure 11. Microscope images at 5.1x magnification of two thermoplastic specimens that were a) dry fatigue-tested and failed at 108,097 cycles and b) fatigue-tested while submerged and failed at 60,657 cycles.

## 4. CONCLUSIONS

Thermoplastic and vinyl ester coupons were static- and fatigue- tested in a load frame equipped with a tank. Half the fatigue-tested coupons were submerged in fresh water. The static-tested flexural strength of the vinyl ester composites was 5% higher than that of the thermoplastic composites. The failure mode for both the vinyl ester and thermoplastic static-tested composites was top ply delamination along the gauge section of the compression side.

In Murdy et al [5], Derakane 411C-350 vinyl ester-epoxy and Hexion 035 epoxy composite T-bolt subcomponents were static and fatigue tested after hydrothermal aging. Murdy et al [5] stated, “contrary to the static strength results, the dry Hexion specimens exhibited much better fatigue lives than their Derakane counterparts. The number of cycles to failure of the dry Hexion specimens was almost two orders of magnitude greater than the dry Derakane specimens” [5].” In this study, despite having flexural strength values that were 5% higher than the thermoplastic composites, the vinyl ester composites had 86% lower cycles to failure than the thermoplastic composites, indicating that higher composite strength does not necessarily indicate higher fatigue life.

Both the cycles-to-failure values and the failure modes differed significantly between vinyl ester and thermoplastic specimens. There were 69% and 42% decreases in cycles to failure from dry to submerged fatigue tests for the vinyl ester and thermoplastic composites, respectively. However, two-tail t-tests with  $\alpha = 0.05$  indicated that the drop from dry to submerged cycles-to-failure averages for the vinyl ester composites was not statistically significant, likely due to the high standard deviations. The drop from dry to submerged cycles-to-failure averages for thermoplastic composites was statistically significant. For dry fatigue tests, the thermoplastic composites had 86% higher cycles to failure than the vinyl ester composites. Two-tail t-tests with  $\alpha = 0.05$  indicated that the higher cycles to failure for dry thermoplastic composites compared to dry vinyl ester composites is statistically significant.

Compared to dry, the submerged fatigue-tested vinyl ester specimens had more permanent changes in shape and more fiber breakage on the tension sides. In addition, dry vinyl ester specimens had more delamination near the supports while submerged vinyl ester specimens had more delamination in the gauge section. Both dry and submerged vinyl ester failed specimens had through-thickness delamination. However, the dry vinyl ester specimens had more fiber bridging through the thickness. The through-thickness delamination in the dry coupons likely occurred from the interlaminar shear stresses between the two fabric plies.

The dry fatigue-tested thermoplastic specimens had more through-thickness delamination failure whereas there was no through-thickness failure for submerged fatigue-tested thermoplastic specimens. The submerged fatigue-tested thermoplastic specimens had top-ply delamination failure. Both dry fatigue-tested vinyl ester and thermoplastic composites had tension-side face sheet delamination. However, the delamination was more severe in the dry fatigue-tested vinyl ester specimens than the thermoplastic specimens.

The submerged fatigue failure modes for the thermoplastic specimens were significantly different than for the vinyl ester specimens. The thermoplastic specimens had compression-side ply delamination, whereas the vinyl ester specimens had permanent deformation after failure and

fiber breakage on the tension sides. The compression-side ply delamination failure in the thermoplastic specimens could indicate that the effect of water ingress on the outer thermoplastic composite surfaces is more substantial than the effect of interlaminar shear stresses during coupon fatigue testing.

Sperling [13] states that thermoset polymers usually do not exhibit any rubber elasticity behavior but does not indicate the difference in rubber elasticity behavior between thermosets and thermoplastics. Further studies of differences in the rubber elasticity behavior between the vinyl ester and thermoplastic resins could explain the significant differences in fatigue properties. Higher elasticity in the thermoplastic resin system could explain the increased cycles to failure and different failure modes in the thermoplastic composites compared to the vinyl ester composites.

## **5. FUTURE WORK**

### **5.1 Planned Future Work**

Planned future work will include continued coupon-scale four-point-bend fatigue testing, coupon-scale water absorption testing, and the development of submerged subcomponent fatigue testing methods. Continued coupon-scale four-point-bend fatigue testing will include submerged Westlake 035c epoxy composites. In both Bharath et al [16] and Murray et al [17], a protective coating called M-Coat JA was applied over strain gauges placed along deployed tidal turbine blades. Continued fatigue research will include an examination of differences in strain results from strain gages that have been coated and not coated with M-Coat JA. Coupon-scale water absorption testing will involve hygrothermally aging vinyl ester, thermoplastic, and epoxy composites and measuring mass changes over time according to [18].

Coupon-scale testing is used for low-cost material parameter characterization, but subcomponent testing is necessary to characterize composite behavior in structural joints and increasingly complex geometries [19]. In Fernandes et al [20], double cantilever beam carbon fiber reinforced polymer specimens adhered with the Araldite 2015 epoxy adhesive that were immersed in distilled water at 50°C for 4 months had decreases in fracture compared to unconditioned specimens, indicating that the adhesive degraded due to water submersion. Adhesives are used in marine energy structural joints and may be susceptible to water intrusion during service, so the combined effects of water intrusion and mechanical fatigue need to be characterized to ensure the long-term durability of adhesive joints in extreme ocean environments. In Murdy et al [5], T-bolt, double-ended-insert subcomponents, and short and oversized beam shear specimens were subjected to saltwater conditioning and structurally validated. The spar is the load-carrying beam component of an axial flow marine turbine blade, so the beam-type subcomponent is another type of subcomponent that merits structural validation. Furthermore, a beam-type subcomponent will be subjected to the combined effects of water intrusion and mechanical fatigue to characterize composite behavior in structural joints. Like this study, where a water tank was configured for testing coupons in the 100 kN and 250 kN load frames, submerged subcomponent fatigue testing will involve configuring a water tank to test subcomponents in NREL's 500 kN load frame.

Besides behavior changes from adhesive joints, differences from cut edge exposure effects are anticipated when scaling up to a beam-type subcomponent. Rocha et al [21] created a representative volume element model that showed how water tends to diffuse along fiber-matrix interfaces more than through bulk resin. It is possible that the differences in cycles to failure that were observed between dry and submerged coupons in this study may be driven by the exposure of the cut coupon side to water ingress. Marine turbine blades in the field, however, may not have cut edges exposed to water. Similarly, submerged beam-type subcomponents will have different amounts of cut edge exposure to water.

## 5.2 Suggested Future Work

Future work that is not currently planned but could be beneficial for understanding the effects of water on composite materials include increasing coupon widths, implementing initial coupon defects, conducting tension-tension fatigue comparisons, conducting direct comparisons to hygrothermally aged four-point bend-tested coupons, conducting submerged saltwater tests, and conducting submerged fatigue testing using less wavy fabrics. In this study, the coupon widths were not deliberately varied and had a standard deviation of 0.18 mm. Increasing coupon widths would change the surface area of the coupons, which could lead to differences in the effects of water ingress on fatigue properties. In coupon testing in particular, high stresses at free edges may be expected to cause delamination in laminates, particularly under fatigue loadings [22]. Moreover, increasing coupon widths might affect free-edge effects.

In this study, there were varied failure initiation locations. To have more consistent failure initiation locations, machined defects such as holes, notches, or pre-cracks could be used. More consistent failure locations would facilitate failure mode comparisons between dry and submerged specimens.

Hygrothermally-aged coupons of the same composite types from this study are currently being tension-tension fatigue-tested at Montana State University. Future work could include comparisons between this study and Montana State University's tension-tension fatigue studies.

In this study, dry and submerged fatigue tests were compared. Future work could include an additional comparison to four-point bend unsubmerged hygrothermally-aged specimens using the same material types. By comparing the submerged specimens to unsubmerged hygrothermally-aged specimens, the effect of water ingress on fatigue crack propagation could be measured. In addition, the necessity of submerged testing compared to sequential hygrothermal testing can be evaluated.

In this study, specimens were submerged in tap water. However, marine energy structures are being considered for ocean environments that consist of salt water and aquatic species. Future research could include fatigue testing in simulated seawater or with the presence of aquatic species to simulate in-service conditions more adequately. Seawater and aquatic species could lead to further degradation of composite materials from salt-buildup and biofouling in fatigue cracks. Saltwater fatigue testing could be challenging, however, as salt would corrode load frame assemblies.



In this study, the unidirectional tows in the Vectorply E-QX 9000 fabric were wavy, which may have contributed to lower and more variable static and fatigue properties than if the unidirectional tows were straight. Future work could include submerged fatigue testing of coupons that include straighter unidirectional tows. Continued work to understand the combined effects of water ingress and mechanical fatigue on composite materials will inform marine energy converter designs and standards, which will reduce reliance on fossil fuels and make marine energy a more viable form of renewable energy.

## 6. ACKNOWLEDGEMENTS

The authors would like to thank David Barnes, Victor Castillo, Ryan Beach, and Collin Sheppard for their excellent support in this project. David Barnes helped with composite panel manufacturing and instruction. Victor Castillo constructed the load frame setup. Ryan Beach helped with the fatigue testing. Finally, Collin Sheppard has provided ongoing guidance for the Marine Energy Advanced Materials project.

This work was authored by the National Renewable Energy Laboratory, operated by Alliance for Sustainable Energy, LLC, for the U.S. Department of Energy (DOE) under Contract No. DEAC36-08GO28308. Funding provided by U.S. Department of Energy Office of Energy Efficiency and Renewable Energy Water Power Technologies Office. The views expressed herein do not necessarily represent the views of the DOE or the U.S. Government. The U.S. Government retains and the publisher, by accepting the article for publication, acknowledges that the U.S. Government retains a nonexclusive, paid-up, irrevocable, worldwide license to publish or reproduce the published form of this work, or allow others to do so, for U.S. Government purposes.

## 7. REFERENCES

1. *Water Power Technologies Office: Multi-Year Program Plan*. 2022: United States.
2. Augustine, C., et al., *Renewable Electricity Futures Study. Volume 2: Renewable Electricity Generation and Storage Technologies. (Volume 2 of 4)*. 2012, National Renewable Energy Laboratory.
3. Hernandez-Sanchez, B.A., et al. *Evaluation of composite materials for wave and current energy technologies*. 2019. United States.
4. Meng, M., et al., *Moisture effects on the bending fatigue of laminated composites*. Composite structures, 2016. **154**: p. 49-60.
5. Murdy, P., et al., *Subcomponent Validation of Composite Joints for the Marine Energy Advanced Materials Project*. 2023.
6. Jiang, Y., et al., *Structural analysis of a fibre-reinforced composite blade for a 1 MW tidal turbine rotor under degradation of seawater*. Journal of ocean engineering and marine energy, 2023. **9**(3): p. 477-494.
7. Boresi, A.P., Schmidt, Richard J, *Advanced Mechanics of Materials*. Sixth ed. 2003, Hoboken, NJ: John Wiley & Sons, Inc.
8. Barbero, E., *Introduction to Composite Materials Design*. Second Edition ed. 2011, Boca Raton, FL: CRC Press.

9. Selvarathinam, A.S. and Y.J. Weitsman, *A shear-lag analysis of transverse cracking and delamination in cross-ply carbon-fibre/epoxy composites under dry, saturated and immersed fatigue conditions*. Composites Science and Technology, 1999. **59**(14): p. 2115-2123.
10. Selvarathinam, A.S. and Y.J. Weitsman, *Transverse cracking and delamination in cross-ply gr/ep composites under dry, saturated and immersed fatigue*. International Journal of Fracture, 1998. **91**(2): p. 103-116.
11. Cousins, D.S., et al., *Recycling glass fiber thermoplastic composites from wind turbine blades*. Journal of Cleaner Production, 2019. **209**: p. 1252-1263.
12. Murray, R.E., et al., *Manufacturing a 9-Meter Thermoplastic Composite Wind Turbine Blade: Preprint*. 2017, National Renewable Energy Laboratory.
13. Sperling, L.H., *Introduction to physical polymer science*. 2006, Wiley: Hoboken, N.J.
14. Lerman, M.W., D.S. Cairns, and J.W. Nelson, *Investigation of the Effect of In-Plane Fiber Waviness in Composite Materials through Multiple Scales of Testing and Finite Element Modeling*. 2017: United States.
15. *D7264/D7264M Standard Test Method for Flexural Properties of Polymer Matrix Composite Materials*. 2015.
16. Bharath, A., et al. *Open Water Blade Strain Measurements on a Vertical-Axis Tidal Turbine*. 2023. United States: New York, NY: American Society of Mechanical Engineers (ASME).
17. Murray, R.E., et al. *Toward the Instrumentation and Data Acquisition of a Tidal Turbine in Real Site Conditions*. 2023. **16**, 1255 DOI: 10.3390/en16031255.
18. International, A., *Standard Test Method for Moisture Absorption Properties and Equilibrium Conditioning of Polymer Matrix Composite Materials*. 2020, ASTM International: West Conshohocken, PA.
19. Gintert, L.A., *Element and Subcomponent Testing*, in *Composites*, D.B. Miracle and S.L. Donaldson, Editors. 2001, ASM International. p. 0.
20. Fernandes, R.L., M.F.S.F. de Moura, and R.D.F. Moreira, *Effect of moisture on pure mode I and II fracture behaviour of composite bonded joints*. International Journal of Adhesion and Adhesives, 2016. **68**: p. 30-38.
21. Rocha, I.B.C.M., et al., *Experimental/numerical study of anisotropic water diffusion in glass/epoxy composites*. IOP Conference Series: Materials Science and Engineering, 2016. **139**(1): p. 012044.
22. Pipes, R.B. and N.J. Pagano, *Interlaminar Stresses in Composite Laminates Under Uniform Axial Extension*. Journal of Composite Materials, 1970. **4**(4): p. 538-548.